A Multiscale Model of a Two-Dimensional Micro-Mirror Array

Nguyen Nhat Binh Trinh[1], Michel Lenczner[1], Frédéric Zamkotsian[2], and Nicolas Ratier[1]

[1]FEMTO-ST, University of Bourgogne Franche-Comté, CNRS, UTBM, ENSMM, Besançon, France.
[2]LAM-CNRS, AMU, Marseille, France.
Email : nhat-binh.trinh@femto-st.fr, michel.lenczner@univ-fcomte.fr, frederic.zamkotsian@lam.fr, nicolas.ratier@femto-st.fr

Abstract

A methodology for the simulation of large two-dimensional micro-mirror arrays (MMA) whose behavior is governed by the static electro-mechanical system is presented. The considered array is actuated by two different voltages in two subdomains. The proposed solution makes it possible to perform simulations of an arbitrarily large size array without resorting to global calculations. It is built using principles derived from periodic homogenization, precisely it is composed of periodic solutions and boundary layer correctors. We discuss the model's interests in its implementation, its simulation and its integration into the MEMSALab software for automated construction of multi-scale models.

Keywords: Micro-Mirror Array, Periodic Homogenization, Boundary Layer Correctors

1. Introduction

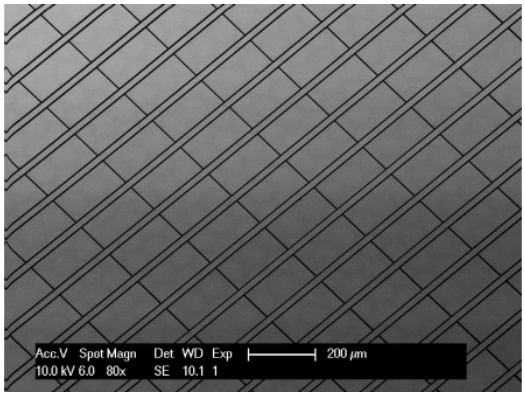

Fig. 1: Top view of the MIRA micro-mirror array when all the mirrors are in the rest position.

Micro-mirror matrices are developed as field selectors for multi-object spectroscopy (MOS) in astrophysics. This observation technique makes it possible to simultaneously collect spectra of faint galaxies and stars in the infra-red and in the visible. The use of field selectors consisting of MOEMS array allows the increase of the number of targets, rapid reprogramming, and should be able to operate in a cryogenic environment. For many years the Laboratoire d'Astrophysique de Marseille (LAM) has developed first in a collaboration with EPFL (Switzerland) and recently together with CSEM (Switzerland) an array of electrostatically actuated tilting mono-crystalline silicon micro-mirrors called MIRA, see its top view in Figure 1. As a field selector for MOS, it has been designed with stringent requirements such as a filling factor of more than 80%, a contrast ratio of more than 1000, a wavelength bandwidth from visible to IR, an actuation voltage lower than 100V and an operating temperature ranging from room temperature to less than 100K, see [12], [3] and [4] for details.

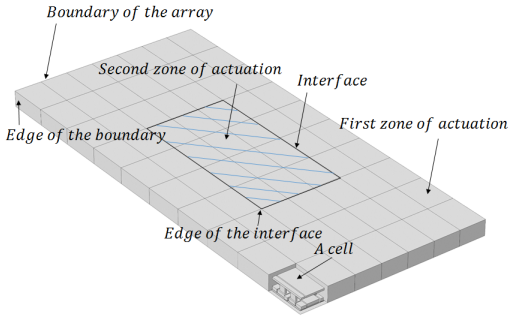

Fig. 2: The two-dimensional array MIRA of micro-mirrors with the two zones of different actuations as well as their interface and the boundaries where the boundary layer terms are added.

This article is a contribution to multi-scale modeling and simulation of this array of micro-mirrors. It follows the article [10] which introduces a model of the electric field in a mono-dimensional MMA with two zones of different actuation. The model includes periodic solutions in both zones that are corrected by boundary layer terms at the zone interfaces as well as at the array ends. They make it possible to guarantee the respect of the boundary conditions and the continuity conditions at interfaces between zones. This model was implemented in COMSOL and showed that the simulation time depends on the numbers of zones and of interfaces but not on the number of cells. Here, the modeling takes into account, in addition to the electrostatic field, the elastic deformations and the electrostatic force still in the quasi-static regime. It is developed for a two-dimensional MMA that also includes two zones of different actuations. The solution still consists of periodic parts in each zone and their boundary layer corrections to the interfaces and the array boundary, see Figure 2. As these corrections are built independently on each face of the interface and of the lateral array boundary, it follows that they produce that the sum of

their contribution is discontinuous at the face junctions, that is to say at the edges. Here, boundary layer correctors are also introduced to these edges. The resulting model is implemented in COMSOL. Here too, the simulation time depends on the number of zones, boundary and interface faces and edges, but not on the number of cells. Thus, it can be applied to an arbitrary large array for a reasonible simulation time.

In addition to the model itself, its construction is an interesting contribution because it has been designed in a way that is consistent with its integration in the MEMSALab software [13], [2], [9] of generation of asymptotic models. This software under development will automatically generate multi-scale multiphysical models for structures with one or more asymptotic characteristics such as periodicity, the thinness of certain substructures or highly heterogeneous coefficients. From a mathematical point of view, model constructions are based on the use of the periodic unfolding method [7], [8], [6], [5]. From the computer science point of view, they are implemented by rewriting techniques. They are expressed according to a so-called extension-combination principle designed to facilitate their reusability.

The rest of the content of the paper is as follows. We first recall the equations of the system and the assumptions used for the construction of the model. Then, we detail the two-scale transformations used for the application of the periodic unfolding method to the construction of each of the components of the model. Then, the implementation of the model in COMSOL is described and simulation results are reported. The implementation in progress in MEMSALab is mentioned before to draw conclusions.

2. The Governing Equations of the MMA

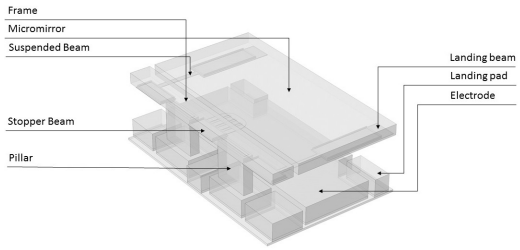

Fig. 3: The parts of a cell of MIRA.

The LAM's micro-mirror array consists in several thousand micro-mirrors cells arranged in a rectangular shape. Each cell has two parts that are assembled as shown on Figure 3. The mirror part is composed of a mirror, a system of beams and a frame. The mirror is attached to the frame by the suspended beams. Two landing beams are on the tips of the suspended beams to prevent the mirror from a short-circuit generation when in contact with the electrode during actuation. A stopper beam placed under the frame provides a precise tilt angle after actuation. The mirror part is with imposed electric potential ϕ at $-V/2$. The electrode part is composed of an electrode, two landing pads and two pillars. The voltage $V/2$ applied to the electrode generates an electrostatic force attracting the micromirror. The two landing pads are the landing regions of the landing beams and the pillars are a stiff link between the frame and the electrode.

The outside of these two parts may consist of air or be empty, in both cases the electric potential is the solution of the Poisson equation $\Delta\phi = 0$. In principle we should consider this equation verified to infinity, but for simplicity it is considered only in a box while the zero normal flux condition $\nabla\phi.\mathbf{n} = 0$ is imposed on its boundary. The base of the micro-mirror as well as the mirror itself are considered rigid. The other parts are considered to be linearly elastic and thus the stress tensor $\boldsymbol{\sigma}$ is governed by the equilibrium equation $-\operatorname{div}\boldsymbol{\sigma} = 0$ and its relation with the linearized tensor of strains $\boldsymbol{\varepsilon}(\mathbf{u})$ is by the Hooke law $\boldsymbol{\sigma} = \mathbf{C}\boldsymbol{\varepsilon}$ where $\mathbf{C}$ is the tensor of elasticity that is supposed to be isotropic. Due to the presence of the electrostatic field, the edges of the elastic and rigid parts are subjected to an electrostatic force that is to say that the normal stress is imposed $\boldsymbol{\sigma}.\mathbf{n} = \mathbf{g}$ where $\mathbf{g} = -\left(\frac{1}{2}\mathbf{E}\cdot\mathbf{D}\right)\mathbf{n} + (\mathbf{n}\cdot\mathbf{E})\,\mathbf{D}^T$ is the electrostatic force exerted in the presence of an electric field $\mathbf{E} = -\nabla\phi$ and the corresponding electric displacement field $\mathbf{D} = \epsilon\mathbf{E}$, ϵ being the dielectric constant. The assumption of strain linearity is justified only for small angles of inclination of the mirrors and will have to be relaxed in a later work.

3. Asymptotic Characteristics of the Model

The modeling presented in this article is based on asymptotic analyzes according to different characteristics of the solution of the above equations. Before any asymptotic analysis, the geometry and the fields are scaled by the characteristic scale L of the array: $\mathbf{x}' := \mathbf{x}/L$, $\phi'(\mathbf{x}') := \phi(\mathbf{x})/L$ and $\mathbf{u}'(\mathbf{x}') := \mathbf{u}(\mathbf{x})/L$ from which results the scaled fields $\mathbf{E}'(\mathbf{x}') = \mathbf{E}(\mathbf{x})$, $\mathbf{D}'(\mathbf{x}') = \mathbf{D}(\mathbf{x})$, $\mathbf{g}'(\mathbf{x}') = \mathbf{g}(\mathbf{x})$, $\boldsymbol{\varepsilon}'(\mathbf{u}')(\mathbf{x}') = \boldsymbol{\varepsilon}(\mathbf{u})(\mathbf{x})$ and $\boldsymbol{\sigma}'(\mathbf{x}') = \boldsymbol{\sigma}(\mathbf{x})$ so that the form of the equations is unchanged by this transformation. In the following, we only work in the scaled configuration but, for the sake of simplicity, we ignore the superscript "′".

The periodicity of the geometry and the large number of cells make it possible to introduce the ratio ε between the size of a cell and the size of the array. It is used as a small parameter in an asymptotic analysis that leads to an asymptotic model in the sense of a large number of cells. During this analysis, it is taken into account that in each cell the part associated with the mirror is connected to the voltage $-V/2$ and that the base is clamped. Assuming that the imposed voltage is of the order of ε, it follows that the potential and the mechanical displacement are of the same order which is expressed by the scaling $V^\varepsilon = \varepsilon\overline{V}^\varepsilon$, $\phi^\varepsilon = \varepsilon\overline{\phi}^\varepsilon$ and $\mathbf{u}^\varepsilon = \varepsilon\overline{\mathbf{u}}^\varepsilon$ where $\overline{V}^\varepsilon$, $\overline{\phi}^\varepsilon$ and $\overline{\mathbf{u}}^\varepsilon$ are in the range of $O(1)$ compared to ε.

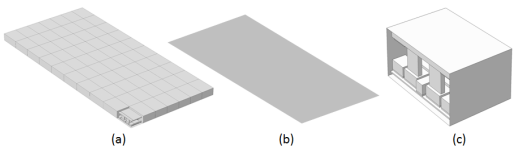

Fig. 4: Elements of the two-scale transformation T^ε: (a) the physical domain made with a periodic array of cells, (b) the macroscopic domain that is a solid two-dimensional section of the array and (c) the microscopic domain obtained by shift and dilation of a cell.

The main part of the two-scale model is obtained by applying the two-scale transformation operator T^ε which

transforms any function defined at the points $\mathbf{x}$ of a block surrounding the micro-mirror array in a function of the variables $\mathbf{x}^\sharp$ of the macroscopic domain which is a two-dimensional section of the block and the variables $\mathbf{x}^1$ of a cell shifted to the origin and dilated by the factor $1/\varepsilon$ see Figure 4 and for instance [8]. This transformation is applied to the three fields $\overline{V}^\varepsilon$, $\overline{\phi}^\varepsilon$ and $\overline{\mathbf{u}}^\varepsilon$ of the model which leads to the expected part of the model after a certain number of operations and the use of the approximations $T^\varepsilon\overline{V}^\varepsilon(\mathbf{x}^\sharp,\mathbf{x}^1) = V^0(\mathbf{x}^\sharp,\mathbf{x}^1)+O(\varepsilon)$, $T^\varepsilon\overline{\phi}^\varepsilon(\mathbf{x}^\sharp,\mathbf{x}^1) = \phi^0(\mathbf{x}^\sharp,\mathbf{x}^1)+O(\varepsilon)$ and $T^\varepsilon\overline{\mathbf{u}}^\varepsilon(\mathbf{x}^\sharp,\mathbf{x}^1) = \mathbf{u}^0(\mathbf{x}^\sharp,\mathbf{x}^1)+O(\varepsilon)$. The main model part is constituted by periodic solutions in each of the two zones of different electric actuation: $\Delta_{\mathbf{x}^1}\phi^0 = 0$ in the air or vacuum part of the reference cell, $\phi^0 = V^0$ on the electrode part, $\phi^0 = 0$ on the mirror part, periodicity conditions on the lateral boundaries and $\nabla_{\mathbf{x}^1}\phi^0.\mathbf{n}_{\mathbf{x}^1} = 0$ on the remaining boundaries of the air/vacuum part.

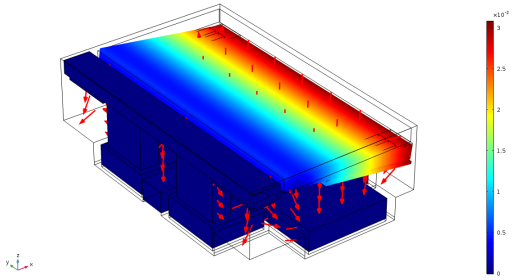

Fig. 5: The vector of electric field $\mathbf{E}^0$ of the main part of the solution, ie the periodic part, is represented by a field of arrows. The applied voltages are ± 30 volts to the mirror part and the electrode part. The vertical mechanical displacements is represented by the deflection of the mirror and is also represented in color.

With regard to the principal mechanical displacement field $\mathbf{u}^0$ and stresses $\boldsymbol{\sigma}^0$, they satisfy the equations $-\operatorname{div}_{\mathbf{x}^1}\boldsymbol{\sigma}^0 = 0$ in the deformable part of the cell and the Hooke law $\boldsymbol{\sigma}^0 = \mathbf{C}\boldsymbol{\varepsilon}^0(\mathbf{u}^0)$ in the variables $\mathbf{x}^1$ of the cell, the clamping condition on the basis of the cell, the normal stress equal to the normalized electrostatic force $\boldsymbol{\sigma}^0.\mathbf{n}_{\mathbf{x}^1} = \mathbf{g}^0$ with $\mathbf{g}^0 = -\left(\frac{1}{2}\mathbf{E}^0\cdot\mathbf{D}^0\right)\mathbf{n} + \left(\mathbf{n}\cdot\mathbf{E}^0\right)\mathbf{D}^{0T}$ where $\mathbf{E}^0 = -\nabla_{\mathbf{x}^1}\phi^0$ and $\mathbf{D}^0 = \epsilon\mathbf{E}^0$, as well as the periodicity conditions on the remaining part of the boundary of the periodicity cell. A simulation result of the electrical field $\mathbf{E}^0$ is shown in Figure 5.

The fields ϕ^0, $\mathbf{D}^0$, $\mathbf{u}^0$ et $\boldsymbol{\sigma}^0$ are defined in the two-scale variables $(\mathbf{x}^\sharp,\mathbf{x}^1)$. They are transported back in the physical domain by the application of the operator B of the inverse two-scale transformation which maps a function defined in the variables $(\mathbf{x}^\sharp,\mathbf{x}^1)$ into a function defined in the physical domain [8]. The resulting fields being periodic in each actuation zone it follows that they are discontinuous at their interface. Corrections are built in the vicinity of each of the interfaces using an asymptotic "boundary layer" method. For this we use an operator T^ε_{BL} of expansion by the factor $1/\varepsilon$ in the direction orthogonal to the interface and of two scale transformation in the transverse directions, see [11] and [9]. It transforms any function defined at the points $\mathbf{x}$ of a neighborhood of the interface into a function of a variable $x^\sharp$ in the macroscopic transverse direction, and of variables $\mathbf{x}^1$ in a column orthogonal to the interface consisting of cells dilated by the factor $1/\varepsilon$.

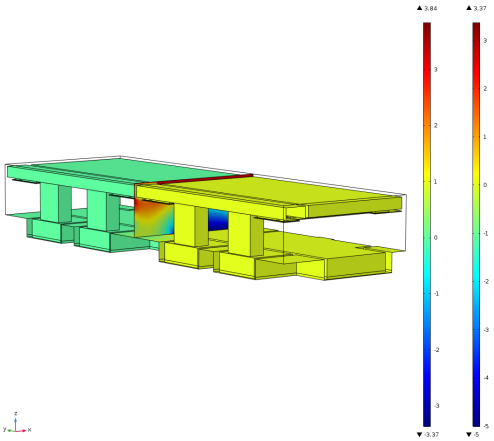

Fig. 6: A column of two dilated cells obtained by a boundary layer two-scale transformation T^ε_{BL} for calculating one of the interface boundary layers. The boundary layer contribution is computed for the electrostatic problem only. The electric potential is represented in colors at the interface.

These operators of boundary layer transformations are applied to the differences between the fields and their main approximation yielding the boundary layer correctors $T^\varepsilon_{BL}(\phi^\varepsilon - B\phi^0) = \phi^0_{BL} + O(\varepsilon)$, $T^\varepsilon_{BL}(\mathbf{u}^\varepsilon - B\mathbf{u}^0) = \mathbf{u}^0_{BL} + O(\varepsilon)$ and $T^\varepsilon_{BL}(\mathbf{g}^\varepsilon - B\mathbf{g}^0) = \mathbf{g}^0_{BL} + O(\varepsilon)$. By construction, these boundary layer fields are evanescent away from the interface. The boundary layer electrical potential ϕ^0_{BL} satisfies $\Delta_{\mathbf{x}^1}\phi^0_{BL} = 0$ in the air or vacuum part of the column of dilated cells, $\phi^0_{BL} = 0$ on the electrode and the mirror parts, the jump conditions $[\![\nabla_{\mathbf{x}^1}\phi^0_{BL}]\!].\mathbf{n}_{\mathbf{x}^1} = -[\![\nabla_{\mathbf{x}^1}\phi^0]\!].\mathbf{n}_{\mathbf{x}^1}$ and $[\![\phi^0_{BL}]\!] = -[\![\phi^0]\!]$ at the interface, the periodicity conditions on the periodic boundaries of the column of cells and $\nabla_{\mathbf{x}^1}\phi^0_{BL}.\mathbf{n}_{\mathbf{x}^1} = 0$ on the remaining boundaries of the air or vacuum part. Figure 6 shows one of the boundary layer corrector ϕ^0_{BL} solution of the above electrostatic boundary value problem. The equations governing the boundary layer mechanical behavior are $-\operatorname{div}_{\mathbf{x}^1}\boldsymbol{\sigma}^0_{BL} = 0$ in the deformable part of the cell and the Hooke's law $\boldsymbol{\sigma}^0_{BL} = \mathbf{C}\boldsymbol{\varepsilon}^0_{BL}(\mathbf{u}^0_{BL})$ in the variables $\mathbf{x}^1$ of the column of dilated cells, the clamping condition on the basis of the cells, the interface jump conditions $[\![\boldsymbol{\sigma}^0_{BL}]\!].\mathbf{n}_{\mathbf{x}^1} = -[\![\boldsymbol{\sigma}^0]\!].\mathbf{n}_{\mathbf{x}^1}$ and $[\![\mathbf{u}^0_{BL}]\!] = -[\![\mathbf{u}^0]\!]$, the correction on the electrostatic force $\boldsymbol{\sigma}^0_{BL}.\mathbf{n}_{\mathbf{x}^1} = \mathbf{g}^0_{BL}$ not detailed here for shortness, and periodicity conditions on the periodicity faces of the column of cells. The boundary layer terms ϕ^0_{BL} and $\mathbf{u}^0_{BL}$ are transported back to the physical space thanks to the application of operators B_{BL} of inverse two-scale boundary layer transformations yielding $B_{BL}\phi^0_{BL}$ and $B_{BL}\mathbf{u}^0_{BL}$ in the vicinity of each face of the interface.

Just as the periodic fields $B\phi^0$ and $B\mathbf{u}^0$ do not satisfy the conditions of continuity at the interfaces between actuation zones, nor do they satisfy the boundary conditions verified by the nominal fields ϕ and $\mathbf{u}$. Thus, boundary layer correctors are constructed at the location of the application of boundary conditions in a manner similar to boundary lay-

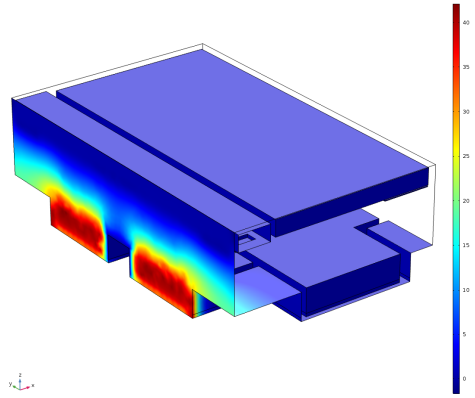

Fig. 7: A boundary layer corrector ϕ^0_{BL} of the electrical potential at a boundary. It is solution of the electrostatic problem not coupled with the mechanical problem. The contribution is very localized but is of the same order of magnitude as that of the imposed voltage.

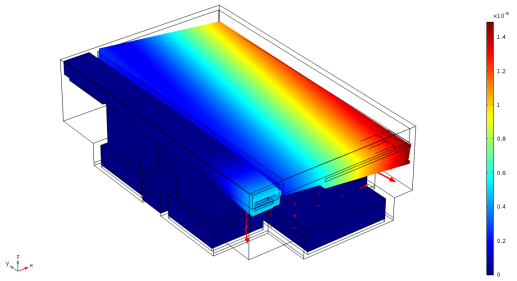

Fig. 8: A boundary layer corrector ϕ^0_{BL}, $\mathbf{u}^0_{BL}$ of the electrical potential and the mechanical displacement, solution of the electro-mechanical problem, at one of the boundaries. The contribution to the mirror deflection is in the range of 5% of the main periodic part.

ers at the interfaces excepted that the load comes from the boundary $\nabla_{\mathbf{x}^1}\phi^0_{BL}.\mathbf{n}_{\mathbf{x}^1} = -\nabla_{\mathbf{x}^1}\phi^0.\mathbf{n}_{\mathbf{x}^1}$ and $\boldsymbol{\sigma}^0_{BL}.\mathbf{n}_{\mathbf{x}^1} = -\boldsymbol{\sigma}^0.\mathbf{n}_{\mathbf{x}^1}$. Figure 7 represents one of the boundary layer corrector ϕ^0_{BL} at one of the boundaries where ϕ^0_{BL} is solution of the electrostatic equations. Figure 8 represents one of the boundary layer corrector pair ϕ^0_{BL}, $\mathbf{u}^0_{BL}$ solution to the above coupled electro-mechanical problem.

In turn, the boundary layer correctors of two interfaces or two adjacent boundaries cause a discontinuity on the edge at their intersection. Thus, for each edge, boundary layer correctors are defined to correct the gap between the two boundary layer correctors on the faces. At each edge, we associate a dilation operator $T^\varepsilon_{BL,edge}$ of expansion ratio $1/\varepsilon$ centered at the center of the edge. It follows the boundary layer corrections $T^\varepsilon_{BL,edge}(\phi^\varepsilon - B\phi^0 - B_{BL,1}\phi^0_{BL,1} - B_{BL,2}\phi^0_{BL,2}) = \phi^0_{BL,edge} + O(\varepsilon)$, $T^\varepsilon_{BL,edge}(\mathbf{u}^\varepsilon - B\mathbf{u}^0 - B_{BL,1}\mathbf{u}^0_{BL,1} - B_{BL,2}\mathbf{u}^0_{BL,2}) = \mathbf{u}^0_{BL,edge} + O(\varepsilon)$ and $T^\varepsilon_{BL,edge}(\mathbf{g}^\varepsilon - B\mathbf{g}^0 - B_{BL,1}\mathbf{g}^0_{BL,1} - B_{BL,2}\mathbf{g}^0_{BL,2}) = \mathbf{g}^0_{BL,edge} + O(\varepsilon)$ where the indices 1 and 2 refer to the two faces Γ_1 and Γ_2 adjacent to the considered edge. By construction, these boundary layer fields are evanescent away from the edge. The equations governing the corrector $\phi^0_{BL,edge}$ are $\Delta_{\mathbf{x}^1}\phi^0_{BL,edge} = 0$ in the air or vacuum part of the dilated cells, $\phi^0_{BL,edge} = 0$ on the electrode and the mirror parts, $\nabla_{\mathbf{x}^1}\phi^0_{BL,edge}.\mathbf{n}_{\mathbf{x}^1} = -\nabla_{\mathbf{x}^1}\phi^0_{BL,1}.\mathbf{n}_{\mathbf{x}^1}$ on the face Γ_2, $\nabla_{\mathbf{x}^1}\phi^0_{BL,edge}.\mathbf{n}_{\mathbf{x}^1} = -\nabla_{\mathbf{x}^1}\phi^0_{BL,2}.\mathbf{n}_{\mathbf{x}^1}$ on the face Γ_1 and $\nabla_{\mathbf{x}^1}\phi^0_{BL}.\mathbf{n}_{\mathbf{x}^1} = 0$ on the remaining boundaries of the air or vacuum part. For shortness, we do not detail the equations verified by the edge boundary layer correctors of the elastic strain field nor those relating to the edges at the interfaces.

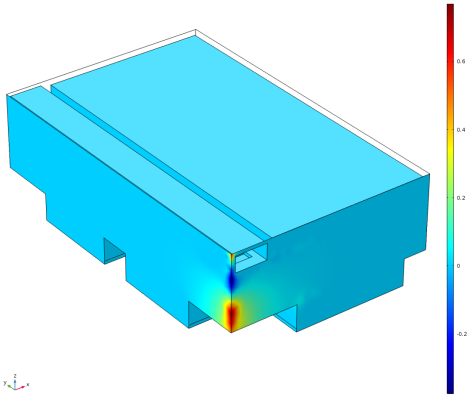

Fig. 9: A solution ϕ_{BL} of the boundary layer problem to an edge. The corrector is for the purely electrostatic problem. We observe that in this case the solution is very localized.

4. Implementation and Simulations

The implementation is done in COMSOL Multiphysics. More precisely, the implementation of the equations of each of the periodic principal parts $(\phi^0, \mathbf{u}^0)$ is carried out with a single cell. The boundary layer correctors $(\phi^0_{BL}, \mathbf{u}^0_{BL})$ are calculated with a single cell for the boundaries and with a column of two cells for the interfaces. For the edge correctors, we use either one cell for the boundary or four cells for the interfaces.

From the point of view of simulation, the characteristics of the above model can be summarized as follows. The model consists of a large number of boundary value problems that are all posed on a small number of cells independent of the size of the array. The solution of the model at a point in the array consists of the main periodic part, possibly corrected by boundary or interface boundary layer correctors and an edge boundary layer correctors. In any case, the contributions are strictly local and do not require any global calculation. Thus, the simulation of a large MMA is done by assembling local contributions computed on a very small number of cells.

In this article we do not present a comparison between the proposed model and a direct simulation of an MMA that would serve as validation. It is nevertheless noted that, in principle, a model obtained by an asymptotic method is all the better if the asymptotic parameter ε is small, ie if the number of cells in the array is large. This principle is validated for all kinds of configurations by a lot of numerical simulation work for problems that are generally much less complex. Moreover, there are also many theoretical articles that show that the error between the solution of the nominal

problem and the periodic solution of the asymptotic model is of the order of $\sqrt{\varepsilon}$ and of the order ε when the boundary layer correctors are taken into account, see for example the reference article [1] for a simpler problem. In the present work, we did not calculate the numerical error between the result of direct simulation of a large MMA and that of our model, because the simulation times and the memory resources for a large array are prohibitive. In addition, we have not yet done the theoretical work of error estimation. Nevertheless, we consider that the method is sufficiently tested to be used without additional justification.

5. Perspectives of Implementation in MEMSALab

The principle of boundary layer correctors is general to all problems of periodic homogenization. In all these problems, the periodic part of the solution does not satisfy either the boundary conditions or the possible interface conditions between zones of the same periodicity. Then a good approximation must include the boundary layer terms. Nevertheless, the number of boundary layer equations to be built is large and their implementation is a long and laborious operation when it has to be developed on a case by case basis. This limits their use in the context of specific model developments. From the point of view of the implementation in the MEMSALab software, the characteristics of the above type of model are as follows. The construction of the boundary layer models follows a method similar to that of the construction of the main part of the model, each part of model requiring a specific two-scale transformation, and therefore fits well with the extension-combination principle. This can be seen through the derivation of the main periodic part of the electrostatic problem and of the boundary layers for a one-dimensional array as detailled in the PhD thesis [9]. The generalization to a two-dimensional MMA and to the electromechanical problem is being drafted. Moreover, the construction of a large number of boundary layer problems does not seem to pose any particular difficulty since it can be automated. To date, the implementation in MEMSALab of automatic building boundary layer problems is in progress.

6. Conclusion

The method that is proposed makes it possible to simulate the solution of the electromechanical problem in a large MMA. The proposed modeling does not require global calculations, but nevertheless makes it possible to calculate the solution at any point of the array, whether in the middle of the array, near the boundary of the array, in the vicinity of the interface between two different zones of different actuation or even to the edges of the boundary or the interface. This solution requires the construction of a large number of boundary layer problems both mathematically and in the simulation tool. Given the regularity of the model construction method, which is based on asymptotic principles, we believe that it is appropriate for its introduction into the MEMSALab software as a general method for correcting periodic parts of homogenized models. This is what we intend to do in the near future. Moreover, calibrations to a MMA in fabrication are planed.

References

1. G. Allaire and M. Amar. Boundary layer tails in periodic homogenization. *ESAIM: Control, Optimisation and Calculus of Variations*, 4:209–243, 1999.
2. W. Belkhir, N. Ratier, D.D. Nguyen, N.N.B. Trinh, M. Lenczner, and F. Zamkotsian. A tool for aided multi-scale model derivation and its application to the simulation of a micro mirror array. In *18th International Conference on Thermal, Mechanical and Multi-Physics Simulation and Experiments in Microelectronics and Microsystems*, pages 1–8. IEEE, 2017.
3. M.D. Canonica. *Large Micromirror Array Based on a Scalable Technology for Astronomical Instrumentation*. PhD thesis, École Polytechnique FéDérale de Lausanne, 2012.
4. M.D. Canonica, F. Zamkotsian, P. Lanzoni, W. Noell, and N. De Rooij. The two-dimensional array of 2048 tilting micromirrors for astronomical spectroscopy. *Journal of Micromechanics and Microengineering*, 23(5):055009, 2013.
5. D. Cioranescu, A. Damlamian, and G. Griso. The periodic unfolding method in homogenization. *SIAM Journal on Mathematical Analysis*, 40(4):1585–1620, 2008.
6. G. Griso. Estimation d'erreur et éclatement en homogénéisation périodique. *Comptes Rendus Mathematique*, 335(4):333–336, 2002.
7. M. Lenczner. Homogénéisation d'un circuit électrique. *Comptes Rendus de l'Académie des Sciences-Series IIB-Mechanics-Physics-Chemistry-Astronomy*, 324(9):537–542, 1997.
8. M. Lenczner and R.C. Smith. A two-scale model for an array of afm's cantilever in the static case. *Mathematical and computer modelling*, 46(5):776–805, 2007.
9. D.D. Nguyen. *Modeling a micro-mirror array and contribution to the development of a simulator of micro-system array*. PhD thesis, Université de Franche-Comté, 2017.
10. D.D. Nguyen, N.N.B. Trinh, M. Lenczner, F. Zamkotsian, and S. Cogan. A model of the electric field in a one-dimensional micro-mirror array and electromechanical simulations and optimization in a single cell. In *18th International Conference on Thermal, Mechanical and Multi-Physics Simulation and Experiments in Microelectronics and Microsystems*, pages 1–5. IEEE, 2017.
11. Thi Trang Nguyen. *Contribution to periodic homogenization of a spectral problem and of the wave equation*. PhD thesis, Besançon, 2014.
12. S. Waldis. *MEMS-based mirror array for astronomical instrumentation*. PhD thesis, Université de Neuchâtel, 2010.
13. B. Yang, W. Belkhir, and M. Lenczner. Computer-aided derivation of multiscale models: A rewriting framework. *International Journal for Multiscale Computational Engineering*, 12(2), 2014.